Anna Rising *et al*. High-yield production of a super-soluble miniature spidroin for biomimetic high-performance materials

ELSEVIER

materialstoday

www.materialstoday.com

NOVEMBER 2021 | VOLUME 50

materialstoday
Connecting the materials community

ELSEVIER

High-yield production of a super-soluble miniature spidroin for biomimetic high-performance materials

Benjamin Schmuck [1], Gabriele Greco [2,3], Andreas Barth [4], Nicola M. Pugno [2,5], Jan Johansson [1], Anna Rising [1,3,*]

[1] Department of Biosciences and Nutrition, Karolinska Institutet, Neo, 141 86 Huddinge, Sweden
[2] Laboratory for Bioinspired, Bionic, Nano, Meta, Materials & Mechanics, Department of Civil, Environmental and Mechanical Engineering, University of Trento, Via Mesiano, 77, 38123 Trento, Italy
[3] Department of Anatomy, Physiology and Biochemistry, Swedish University of Agricultural Sciences, Uppsala, Sweden
[4] Department of Biochemistry and Biophysics, Svante Arrhenius väg 16C, Stockholm University, 10691 Stockholm, Sweden
[5] School of Engineering and Materials Science, Queen Mary University of London, Mile End Road, London E1 4NS, United Kingdom

The mechanical properties of artificial spider silks are approaching a stage where commercial applications become realistic. However, the yields of recombinant silk proteins that can be used to produce fibers with good mechanical properties are typically very low and many purification and spinning protocols still require the use of urea, hexafluoroisopropanol, and/or methanol. Thus, improved production and spinning methods with a minimal environmental impact are needed. We have previously developed a miniature spider silk protein that is characterized by high solubility in aqueous buffers and spinnability in biomimetic set-ups. In this study, we developed a production protocol that resulted in an expression level of >20 g target protein per liter in an *Escherichia coli* fed-batch culture, and subsequent purification under native conditions yielded 14.5 g/l. This corresponds to a nearly six-fold increase in expression levels, and a 10-fold increase in yield after purification compared to reports for recombinant spider silk proteins. Biomimetic spinning using only aqueous buffers resulted in fibers with a toughness modulus of 74 MJ/m^3, which is the highest reported for biomimetically as-spun artificial silk fibers. Thus, the process described herein represents a milestone for the economic production of biomimetic silk fibers for industrial applications.

Keywords: Artificial spider silk; Spidroins; Bioreactor cultivation; Recombinant protein expression

Introduction

The favorable mechanical properties (high strength, yet extensible) and the biocompatible and biodegradable nature [1–4] of spider silk have triggered a quest to harness this material for various industrial applications. Unfortunately, the production of native silk is not feasible on large scale due to the territorial and cannibalistic behavior of spiders [5]. Hence, there is a need for economically feasible large-scale production methods of spider silk proteins (spidroins) using heterologous hosts [6]. Recently, Edlund and co-workers have shown that an economically viable production method using an *Escherichia coli* (*E. coli*) fermentation process and immobilized metal affinity chromatography for protein purification would require an expression level of 10 g/l, enabling a sale price of 23$/kg for artificial spider silk [7].

Spidroins are large proteins (250–350 kDa) and consist of three distinct domains [8]. The poly-alanine/glycine-rich repeat region is embedded between the N-terminal (NT) [9] and the C-terminal (CT) domains [10], both of which respond with

* Corresponding author.
E-mail address: Rising, A. (anna.rising@ki.se)

conformational changes to a pH gradient along the spiders spinning duct [10–13]. This pH dependency of NT and CT together with shear forces trigger the assembly of the spidroins into mature silk fibers.

The presence of the highly repetitive region between NT and CT, containing up to a hundred tandem repeats, makes a high-yield recombinant expression of native spidroins difficult to achieve [14,15] due to limitations of the translation machinery of bacterial hosts [16–18]. To attenuate these constraints codon optimization and upregulating ^{glycyl}tRNA are suggested as effective countermeasures [14,18–21]. Applying this strategy for expressing spidroins in *E. coli* resulted in the highest expression level reported thus far using a bioreactor (3.6 g/l, Table 1), though it should be noted that this is before protein purification and does not reflect the final yield. In addition to the relatively low yields, the recombinant spidroins are prone to aggregate, which is why common techniques to prepare the spinning solutions (dopes) include the use of denaturing agents like urea/guanidium for the re-suspension of inclusion bodies, hexafluoroisopropanol (HFIP) for solubilizing lyophilized proteins, and methanol/isopropanol as a coagulation agent for spinning [14,19,22,23]. Fibers produced using these methods have reached the toughness modulus of native spider silk, provided that additional manual post-spin stretching is applied [14,19,22]. Nevertheless, these harsh conditions are very different from the conditions spiders use to make silk [13,24] and leave the process expensive and harmful to the environment [7,25].

To push the yield to the economically viable level of 10 g/l, we speculated that the designed mini-spidroin NT2RepCT (two natural tandem repeat units flanked by the terminal domains) known for its high solubility of up to 500 mg/ml in aqueous buffers and proper response to lowered pH in biomimetic spinning set-ups [26–29] (Fig. 1a–c), is a suitable candidate for expression in a high-cell density culture. In support of this, bacterial shake-flask cultivations employing the standard *E. coli* BL21 (DE3) strain express NT2RepCT with a yield in a range above 100 mg/l [26], which is a good starting point for further optimizations.

Results and discussion

Our initial attempt to produce NT2RepCT in a high-cell density culture (batch 150I) relied on our previous expression protocols for shake-flasks [26] and a semi-defined cultivation medium with glycerol as the main carbon source suggested by da Silva and co-workers [30]. Thus, compared to the shake-flask protocol we implemented several adjustments for the expression of NT2RepCT in the bioreactor. First, instead of LB-medium, we used a complex growth medium combined with trace metals, phosphate buffer, and an additional carbon source (glucose and glycerol). Second, protein expression was first induced when the optical density at 600 nm (OD_{600}) was >50, instead of around 1. Third, to enable continued growth we implemented a fed-batch setup, with glycerol as the main feed [31].

Briefly, the culture was grown at 25 °C, before the temperature was decreased to 20 °C when OD_{600} reached 50, and protein expression was induced with IPTG (150 μM). Feeding with 40% glycerol started automatically once the initial carbon source (a combination of glycerol and glucose) was depleted (see Fig. S1 for the cultivation plots). After ~30 h pO_2 suddenly spikes, indicating that the depletion of the carbon source. When using this protocol, 22 h after induction NT2RepCT reached an expression level of 13.2 g/l in batch 150I.

Next, we wanted to investigate if moderately higher IPTG concentration for induction would increase the protein yield, and likewise monitor how NT2RepCT accumulates after induction (Fig. 2). To reduce the stress on the culture and enable continued growth [32,33], we decided not to apply higher IPTG concentrations than 250 μM. Independent of the IPTG concentration used for inducing protein expression (150, 200, or 250 μM, named batch 150I_2, 200I, and 250I, respectively), 20 h after induction a plateau is reached with respect to the protein yield (Fig. 2b). The highest NT2RepCT expression level was obtained with 250 μM IPTG, which gave 15.9 g/l (Fig. S2). However, a correlation between the expression level and the IPTG concentration in the tested range could not be observed (Fig. 2b), which means that the differences are most likely attributed to experimental batch-to-batch variations rather than differences in IPTG concentrations (compare also batch 150I and 150I_2, Table S1).

Finally, the cultivation of *E. coli* expressing NT2RepCT was repeated once more but using a larger reactor vessel (final cultivation volume 1.6 l, batch 150IL). Since IPTG can be toxic to the cells [34] and since we did not observe an improved final protein yield when using higher IPTG concentrations (Table S1), we chose to continue to induce the cultures with 150 μM IPTG. Initially, the bacteria were allowed to grow at 29 °C to OD_{600} of 77, before reducing the temperature to 20 °C for induction. 21 h after induction, the culture accumulated an impressive 20.9 g/l of NT2RepCT (estimated with SDS PAGE Table 1, Fig. 1d, and

TABLE 1

Spidroin expression with *E. coli* using a bioreactor.

Culture size (l)	Spidroin[a]	Expression level (g/l)	Yield after purification (g/l)	Size (kDa)	Solubility after expression	Solvent[b]	Reference
2–5	11R26	n.r.	1.5	18	6 M urea	HFIP	[20]
2	96-mer	1.8	n.r.	290	8 M urea	HFIP	[19]
2	32-mer	2.7	1.2	100	8 M urea and 2 M thiourea	HFIP	[14]
~2	MaSp2	3.6	n.r.	202	buffer[c]	n.a.[d]	[21]
1.6	NT2RepCT	20.9	14.5	33	20 mM Tris, pH 8	n.a.	this study

n.r. – not reported. n.a. – not applicable. a) The spidroin names reported in this table correspond to names reported in the listed references. For instance, "32-mer" means that the spidroin contains 32 tandem repeat units of poly-alanine/glycine-rich regions. MaSp 2 contains 64 iterated consensus repeats and the minispidroin NT2RepCT has 2 tandem repeat units and both terminal domains. b) Solvent used to resolubilize lyophilized artificial spidroins after purification. c) The composition of the buffer is not reported. d) The MaSp2 expressed in this study was not purified, and not used for spinning artificial silk.

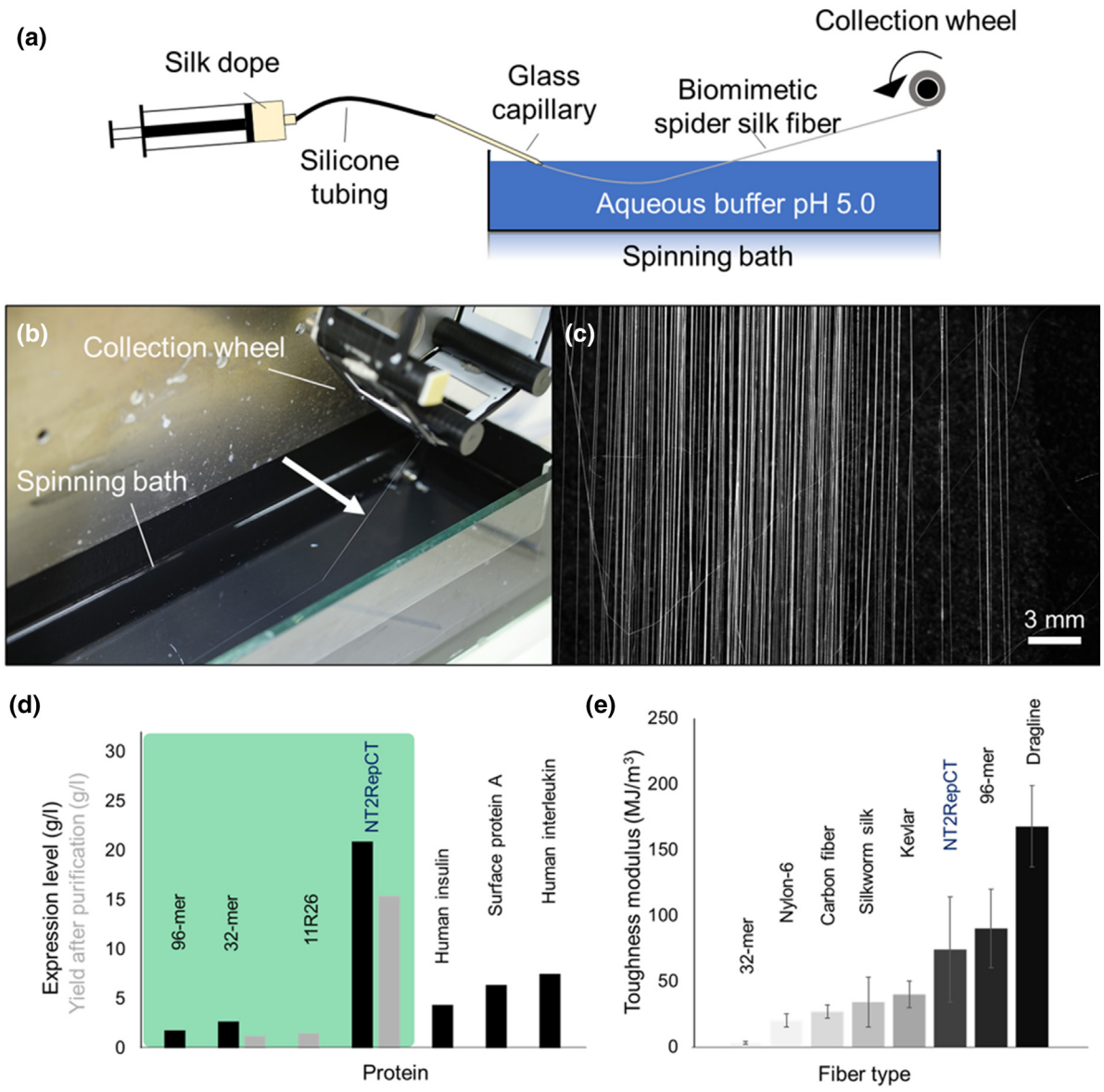

FIGURE 1

Biomimetic spinning setup used to spin the minispidroin NT2RepCT, and comparison of the expression level, yield after purification, as well as the toughness modulus of produced artificial silk with reference proteins/materials. (a) Schematic image of biomimetic spinning: A concentrated solution of NT2RepCT (dope; protein concentration 300 mg/ml in mild aqueous buffer, pH 8) is extruded through a glass capillary into a spinning bath containing an aqueous buffer, pH 5. The pH change and shear forces mimic the conditions of native silk spinning and induce immediate fiber formation. (b, c) The fibers are collected continuously on a collection wheel with a speed of 46 cm s^{-1} (See also Supplementary Video 1). (d) Comparison of the expression level and yield after purification of artificial spidroins (highlighted in green) that were previously expressed using *E. coli* in bioreactor cultivations (96-mer see Ref. [19], 32-mer see Ref. [14], silk protein 11R26 see Ref. [20], and more details in Table 1). As a reference, the graph also includes the highest (to the best of our knowledge) reported expression yields using *E. coli* for human insulin [47], human interleukin-6 [48], and surface protein A (SpaA) from *Erysipelothrix rhusiopathiae* [30]. (E) The toughness modulus of NT2RepCT fibers (this study) compared to fibers from artificial spidroins 96-mer and 32-mer [14,19]; synthetic fibers Nylon 6 [49], Kevlar (see method section in Supporting Information), and Carbon fibers (see method section in Supporting Information); silkworm silk[50], and native dragline spider silk [4].

Fig. S3. The expression level was also estimated considering the dry cell weight to 20.8 g/l. See Fig. S4 and Table S1). A summary of the cultivation parameters and yields is found in Table S1.

The improved cultivation conditions in combination with the relatively small size (33 kDa) and the high solubility of NT2RepCT are likely reasons for the high expression level after culture harvest. Of note, the high solubility of NT has been exploited to develop a tool for the production of aggregation-prone proteins at large [35–39] and could contribute to high yield and solubility also for NT2RepCT. The resulting 20.9 g/l is nearly a 6-fold increase compared to previous bioreactor cultivations of spidroins [14,19,20,21], and twice the level that has been judged economical for commercialization of recombinant silk-based products [7]. In fact, this is among the highest protein expression levels reported to date for *E. coli* produced proteins [30,40–42].

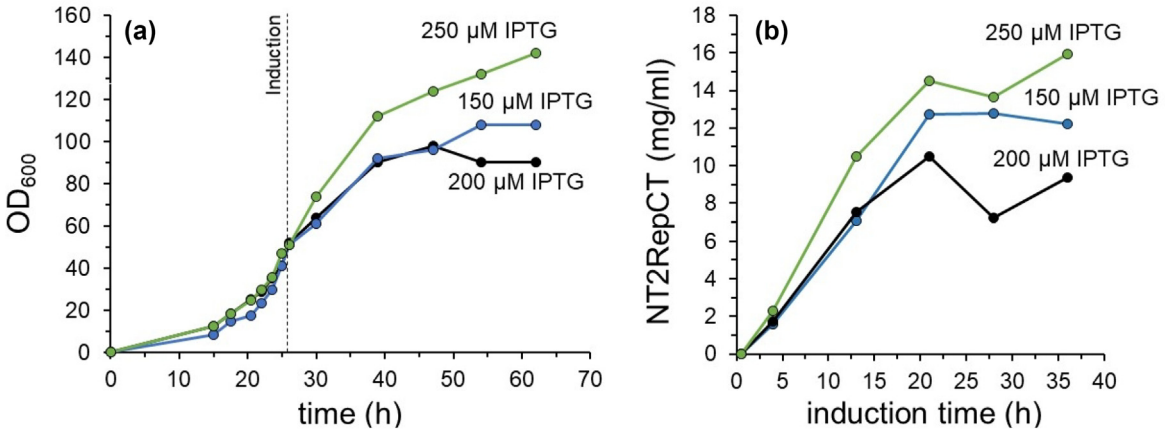

FIGURE 2

Expression of NT2RepCT in *E. coli* in a high-cell density culture (0.35 l) using different IPTG concentrations. (a) OD_{600} of the *E. coli* culture over time before and after induction. The induction point is indicated by the dashed line. (b) The concentration of NT2RepCT in the culture was estimated with SDS-PAGE as a function of induction time.

The downstream processing required no denaturing agents or organic solvents, which makes the entire procedure sustainable and environmentally friendly. After cell lysis using a 20 mM Tris-HCl buffer at pH 8, an insignificant amount of NT2RepCT remained in the pellet after centrifugation (Fig. 3a), and ~95% of NT2RepCT was present in the cell lysate. The target proteins bound efficiently to the columns and the minimum concentration of imidazole required to elute NT2RepCT was investigated

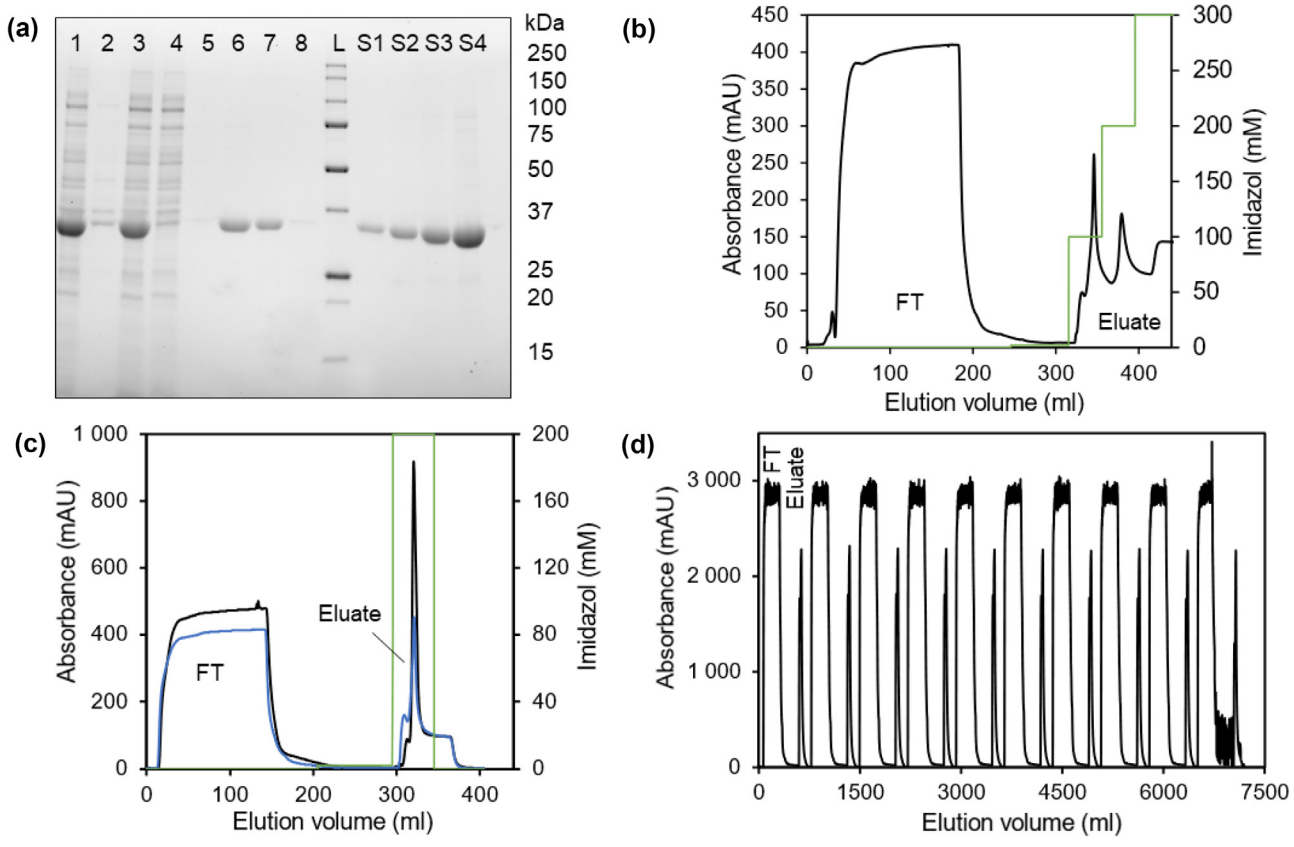

FIGURE 3

Purification of NT2RepCT expressed in the bioreactor using IMAC. (a) SDS-PAGE of lane 1: Total cell content (2-fold dilution); 2: pellet after centrifugation (2-fold dilution); 3: lysate (2-fold dilution); 4: flow-through (2-fold dilution); 5: wash 5 mM imidazole; 6: 100 mM imidazole (10-fold dilution); 7: 200 mM imidazole (10-fold dilution); 8: 300 mM imidazole; l: Ladder. S1–S4 reference samples of NT2RepCT. S1: 0.225 mg/ml; S2: 0.45 mg/ml; S3: 0.9 mg/ml; S4: 1.8 mg/ml. (b) Step elution of protein (black line) from a 20 ml HisPrep FF 16/10 with 100-, 200-, and 300-mM imidazole (green line). (C) Purification of NT2RepCT (batch 250l) with 20 ml HisPrep FF 16/10 (blue line) or HiTrap Chelating HP four-time 5 ml sequentially coupled columns (black line). (D) Processing large quantities of lysate, by using a fully automated protocol for repeated loading and elution (batch: 150lL).

by using a step gradient, which included 100-, 200-, and 300-mM imidazole (Fig. 3b). While most NT2RepCT eluted with 100 mM imidazole, elution with 200 mM was essential to maximize the yield. Next, we compared the purification of NT2RepCT with either 4x5ml HiTrap Chelating HP sequentially coupled columns or a 20 ml HisPrep FF 16/10 column to test if the choice of the column influenced the yield (Fig. 3c). The yield using the HiTrap column was estimated to 11.2 g/l, which is indistinguishable from 11.4 g/l, estimated with the HisPrep column.

Since the columns have a theoretical maximal binding capacity of only 500–800 mg/20 ml medium, we had to establish an automated protocol for repeated loading of lysate and elution of protein to purify more than just a fraction of each batch (Fig. 3d, see SDS-PAGE gel image of the purification in Fig. S5). This made storage of the eluate for longer periods in the cold (6 °C up to 24 h) indispensable. Unexpectantly, the eluate indeed remained clear, and no protein aggregation was observed during the storage of the centrifugated lysate. By using the automated purification procedure, 14.5 g/l NT2RepCT was obtained from batch 150IL, which is 10 times higher than previously reported for recombinant spidroins (Table 1, Fig. 1d). Independent of the batch, purification recovered approximately 70% of the total expressed protein. Thus, the herein achieved production levels and yields after purification, as well as the protein solubility and stability during expression and purification, are unprecedented when comparing to previously published spidroin production protocols (Table 1, Fig. 1d).

Biomimetic spinning was performed using a custom-made device that extruded a concentrated NT2RepCT solution (dope) with a pump-driven syringe through a pulled glass capillary into an aqueous buffer (500 mM Na-acetate, 200 mM NaCl, pH 5) (Fig. 1a–c) [26]. The silk formed immediately once the dope entered the spinning buffer and was collected in air on a rotating wheel placed at the end of the 80 cm long bath. This spinning process is continuous (Supplementary Video 1) and was carried out for several minutes but could in principle be extended to several hours. From one bioreactor culture (1.6 l), 23 g of pure NT2RepCT was obtained, which is enough to prepare 77 ml dope (300 mg/ml). Considering the flow rate for spinning (17 μl/min) and a reeling speed of 46 cm s^{-1}, this amount is enough to spin continuously for 75 h, which corresponds to a 125 km long fiber.

A closer investigation revealed that fibers made from NT2RepCT produced in the bioreactor (batch 150I, 250I, and 150IL) had diameters of <12 μm and the morphology was similar to previously reported fibers made from NT2RepCT produced in shake flasks [26,43,44]. SEM revealed that the fibers are smooth from one side and possess a longitudinal groove along the other side. Under a light microscope, they appeared as straight, twisted, or exhibited a longitudinal groove (Fig. 4 and Fig. S6 for representative micrographs), which are common morphologies of synthetic artificial silk fibers [19,45].

A potential problem for commercial applications of artificial silk fibers is the inherent variability in mechanical properties, which can be observed even for fibers that are spun from the

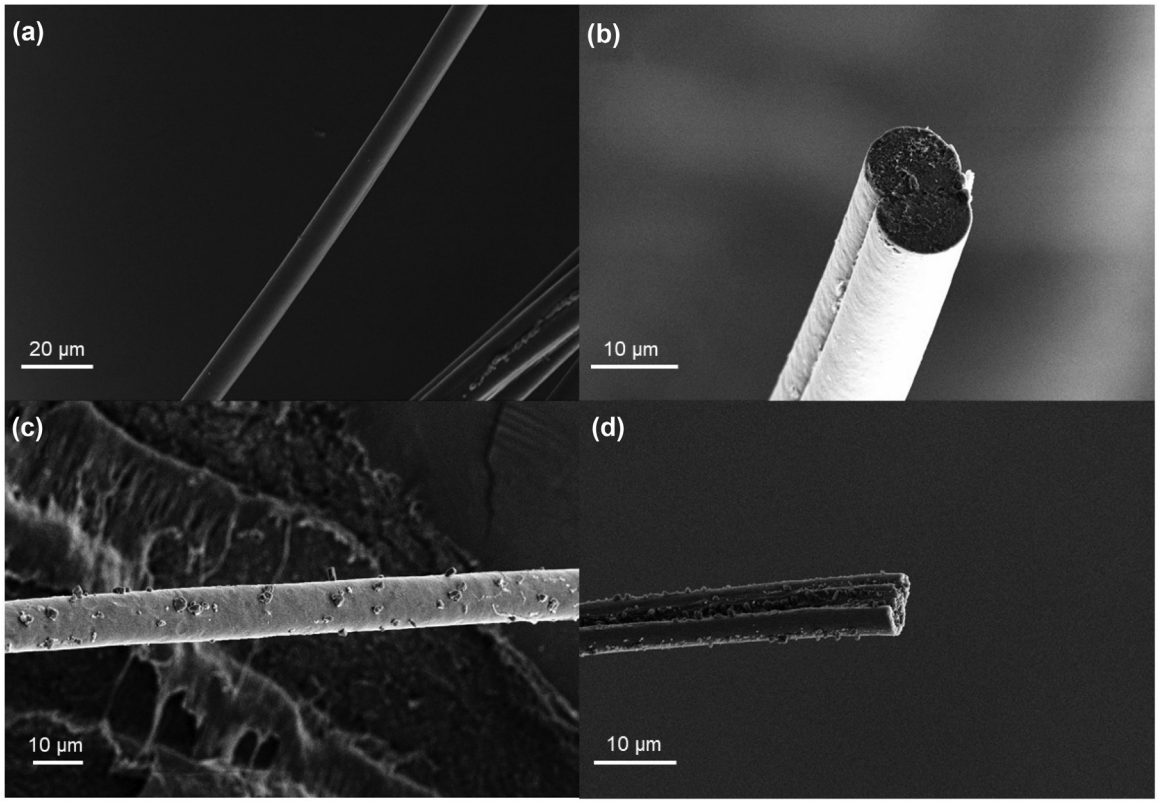

FIGURE 4

Representative SEM images show uniform fibers with a smooth surface on one side and a longitudinal groove on the other side. (a and b) Representative images of fibers which were spun using NT2RepCT from batch 150I. (c and d) Representative images of fibers spun with NT2RepCT from batch 250I.

TABLE 2

Mechanical properties of biomimetic silk fibers from NT2RepCT expressed in the bioreactor.

Batch	Diameter (μm)	Strain at break (%)	Toughness modulus (MJ m^{-3})	Strength (MPa)	Young's modulus (GPa)
150I	11.5 ± 2.1	94% ± 36%	74 ± 40	99 ± 29	2.5 ± 0.7
250I	8.1 ± 2.6	86% ± 29%	70 ± 35	101 ± 30	2.8 ± 0.9
150IL	7.0 ± 1.2	87% ± 17%	64 ± 16	95 ± 20	2.2 ± 0.6

20 fibers were tested for each set. Outliers were not removed.

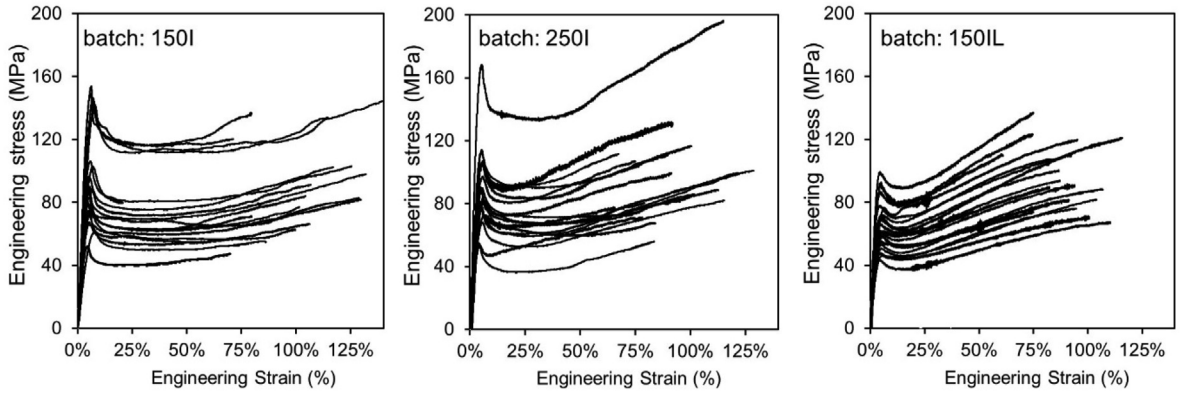

FIGURE 5

Stress–strain curves of NT2RepCT fibers produced in this study. For each set of fibers, 20 randomly selected fibers were tested. Outliers were not removed. The data shown were smoothed to reduce the noise with a moving average function in Microsoft Excel®.

same recombinant protein [26,27,43,44]. The most likely explanation for these variations are subtle differences in the spinning methods used in the respective studies, e.g., size and shape of the capillary nozzle, speed of fiber collection, and time the fiber spends in the bath before being collected in air. Thus, we spun fibers from batch 150I, 250I, and 150IL paying meticulous attention to provide identical spinning conditions. NT2RepCT was spun using a dope extrusion speed of 17 μl/min, a capillary opening diameter of 35 ± 5 μm, and 80 rpm collection wheel speed (46 cm s^{-1} silk fiber collection speed) with the wheel positioned at the end of the 80 cm long bath. Our results show that NT2RepCT produced from three different batches, purified with different columns, and spun at different occasions exhibit mechanical properties that are indistinguishable from each other. The fibers are very extensible (strain at break ~90%), have a significant strength of around 100 MPa, a Young's modulus of ~2.7 GPa, and a toughness modulus of 70 MJ m^{-3} (Table 2 and Fig. 5). The average toughness modulus value between the batches varied by less than ±8%. Also, the Fourier Transform Infrared (FTIR) spectra (Fig. 6 and Fig. S7) of fibers from batch 150I and 250I are very similar in the amide I region and showed that the β-sheet content in both samples is ~40%.

The fibers produced using the herein described method have higher strength and toughness modulus compared to previously described as-spun (without post-spin stretching) artificial silk fibers [26,27,43]. Compared to native dragline silk, the toughness modulus of NT2RepCT fibers is around 50%, and compared to artificial silk fibers that have been produced from recombinant spidroins with reported expression levels >1.5 g/l, the toughness modulus is equal or significantly higher (Fig. 1e). The large protein yields and practically feasible spinning method are important stepping-stones for further improving the fiber properties, e.g. by protein engineering approaches [46].

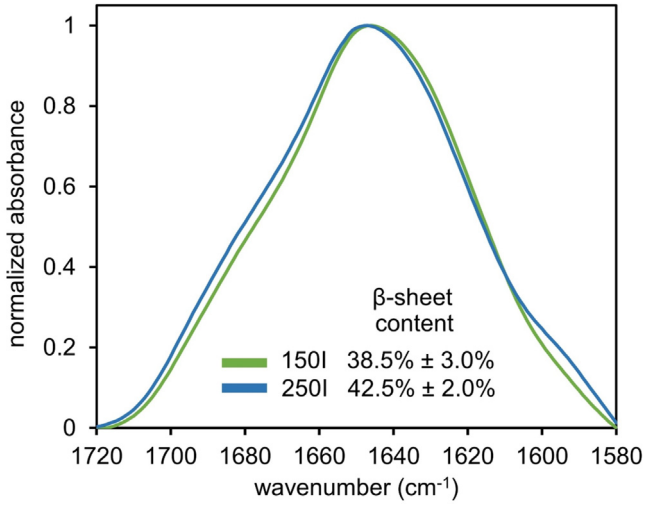

FIGURE 6

FTIR spectra of fibers from NT2RepCT (batch 150I and 250I), in the amide I region (1700–1600 cm^{-1}). The spectra were baseline subtracted and normalized. A detailed description of the secondary structure analysis is provided in the SI and illustrated in Fig. S7.

Concluding remarks

This study describes a protocol for expressing NT2RepCT with an *E. coli* fed-batch culture that yields more than 14 g/l of pure protein. The protocol is surprisingly simple: a standard *E. coli* strain and expression vector was used together with an optimized

cultivation medium composition but without the need of upregulating ^{glycyl}tRNA. In the race to make the production of artificial spider silk economically feasible, this is an important step forward. According to a previously published study the expression levels of artificial spider silk proteins must reach 10 g/l to enable a sale price of 23$/kg for artificial spider silk fibers [7]. The process used for the cost estimation was similar to our method in the expression and down-stream purification parts, but included the use of organic solvents for fiber spinning. The high spidroin expression level reported herein (~20 g/l) combined with the use of solely aqueous buffers for fiber spinning vouch for economically feasible production costs.

Furthermore, the biomimetic spinning setup reported in this study resulted in fibers with reproducible mechanical properties, exhibiting a higher toughness modulus and strength than any previously reported as-spun biomimetic spider silk fiber.

Materials and methods

A detailed description of the methodology used in this study including all references are described in the Supplementary information, available online. There, a description of how the bioreactor cultivations were carried out, the exact purification protocol, the biomimetic spinning procedure, and fiber characterization techniques are found.

Funding details

This work was supported by European Research Council (ERC) under the European Union's Horizon 2020 research and innovation program (grant agreement No 815357), the Center for Innovative Medicine (CIMED) at Karolinska Institutet and Stockholm City Council, Karolinska Institutet SFO Regen (FOR 4-1364/2019), the Swedish Research Council (2019-01257), Olle Engkvist stiftelse (207-0375), and Formas (2019-00427). N. M. P. is supported by the European Commission under the FET Proactive ("Neurofibers") grant No. 732344 as well as by the Italian Ministry of Education, University and Research (MIUR) under the "Departments of Excellence" grant l. 232/2016, the ARS01-01384-PROSCAN and the PRIN-20177TTP3S grants. G. G. is supported by Caritro Foundation (prot. U1277.2020/SG.1130), and by Olle Engkvist stiftelse.

CRediT authorship contribution statement

Benjamin Schmuck: Conceptualization, Methodology, Validation, Investigation, Writing – original draft, Writing - review & editing, Visualization. **Gabriele Greco:** Validation, Investigation, Writing - review & editing, Visualization. **Andreas Barth:** Validation, Resources, Writing - review & editing. **Nicola M. Pugno:** Writing - review & editing, Funding acquisition, Resources. **Jan Johansson:** Writing - review & editing, Supervision, Funding acquisition, Resources. **Anna Rising:** Conceptualization, Methodology, Writing - review & editing, Supervision, Funding acquisition, Resources.

Declaration of Competing Interest

The authors declare that they have no known competing financial interests or personal relationships that could have appeared to influence the work reported in this paper.

Acknowledgements

The authors thank Mats Sandgren, who provided the bioreactor infrastructure located at the Biocentrum, Swedish University of Agricultural Sciences, Uppsala, Sweden. The authors would like to thank Lorenzo Moschini, Prof. Antonella Motta, and Prof. Claudio Migliaresi (Biotech – Mattarello, University of Trento) for their support with the SEM facility.

Declaration of competing interest

No potential conflict of interest was reported by the author(s).

Data availability

The raw data of the results presented in this study are available through the corresponding author on reasonable request.

Appendix A. Supplementary data

Supplementary data to this article can be found online at https://doi.org/10.1016/j.mattod.2021.07.020.

References

[1] C. Radtke et al., PLoS One 6 (2011) e16990, https://doi.org/10.1371/journal.pone.0016990.
[2] C. Allmeling et al., Cell Prolif. 41 (2008) 408–420, https://doi.org/10.1111/j.1365-2184.2008.00534.x.
[3] I. Agnarsson, M. Kuntner, T.A. Blackledge, C. Lalueza-Fox, PLoS One 5 (2010) e11234, https://doi.org/10.1371/journal.pone.0011234.
[4] G. Greco, N.M. Pugno, Molecules 25 (2020) 2938, https://doi.org/10.3390/molecules25122938.
[5] D.H. Wise, Annu. Rev. Entomol. 51 (2006) 441–465, https://doi.org/10.1146/annurev.ento.51.110104.150947.
[6] G. Bhattacharyya et al., Protein Expr. Purif. 183 (2021) 105839, https://doi.org/10.1016/j.pep.2021.105839.
[7] A.M. Edlund et al., N. Biotechnol. 42 (2018) 12–18, https://doi.org/10.1016/j.nbt.2017.12.006.
[8] N.A. Ayoub et al., PLoS One 2 (2007) e514, https://doi.org/10.1371/journal.pone.0000514.
[9] A. Rising et al., Biomacromolecules 7 (2006) 3120–3124, https://doi.org/10.1021/bm060693x.
[10] F. Hagn et al., Nature 465 (2010) 239–242, https://doi.org/10.1038/nature08936.
[11] G. Askarieh et al., Nature 465 (2010) 236–238, https://doi.org/10.1038/nature08962.
[12] N. Kronqvist et al., Nat. Commun. 5 (2014) 3254, https://doi.org/10.1038/ncomms4254.
[13] M. Andersson et al., PLoS Biol. 12 (2014), https://doi.org/10.1371/journal.pbio.1001921 e1001921.
[14] X.X. Xia et al., Proc. Natl. Acad. Sci. U. S. A. 107 (2010) 14059–14063, https://doi.org/10.1073/pnas.1003366107.
[15] A. Rising et al., Cell. Mol. Life Sci. 68 (2011) 169–184, https://doi.org/10.1007/s00018-010-0462-z.
[16] V.G. Debabov, V.G. Bogush, ACS Biomater. Sci. Eng. 6 (2020) 3745–3761, https://doi.org/10.1021/acsbiomaterials.0c00109.
[17] M.B. Hinman, J.A. Jones, R.V. Lewis, Trends Biotechnol. 18 (2000) 374–379, https://doi.org/10.1016/S0167-7799(00)01481-5.
[18] S.R. Fahnestock, S.L. Irwin, Appl. Microbiol. Biotechnol. 47 (1997) 23–32, https://doi.org/10.1007/s002530050883.
[19] C.H. Bowen et al., Biomacromolecules 19 (2018) 3853–3860, https://doi.org/10.1021/acs.biomac.8b00980.
[20] H. Zhang et al., Prep. Biochem. Biotechnol. 46 (2016) 552–558, https://doi.org/10.1080/10826068.2015.1084637.
[21] Y.X. Yang et al., Process Biochem. 51 (2016) 484–490, https://doi.org/10.1016/j.procbio.2016.01.006.
[22] A. Heidebrecht et al., Adv. Mater. 27 (2015) 2189–2194, https://doi.org/10.1002/adma.201404234.
[23] A. Koeppel, C. Holland, ACS Biomater. Sci. Eng. 3 (2017) 226–237, https://doi.org/10.1021/acsbiomaterials.6b00669.

[24] A. Rising, J. Johansson, Nat. Chem. Biol. 11 (2015) 309–315, https://doi.org/10.1038/nchembio.1789.
[25] J.J. Milne, Scale-up of protein purifi cation: Downstream processing issues, Methods Mol. Biol., 2017: 71–84. https://doi.org/10.1007/978-1-4939-6412-3_5.
[26] M. Andersson et al., Nat. Chem. Biol. 13 (2017) 262–264, https://doi.org/10.1038/nchembio.2269.
[27] N. Gonska et al., Biomacromolecules 21 (2020) 2116–2124, https://doi.org/10.1021/acs.biomac.0c00100.
[28] M. Landreh et al., Chem. Commun. 53 (2017) 3319–3322, https://doi.org/10.1039/C7CC00307B.
[29] M. Otikovs et al., Angew. Chem. Int. Ed. 56 (2017) 12571–12575, https://doi.org/10.1002/anie.201706649.
[30] A.J. da Silva et al., Springerplus 2 (2013) 1–12, https://doi.org/10.1186/2193-1801-2-322.
[31] M.A. Eiteman, E. Altman, Trends Biotechnol. 24 (2006) 530–536, https://doi.org/10.1016/j.tibtech.2006.09.001.
[32] Y. Sevastsyanovich et al., FEMS Microbiol. Lett. 299 (2009) 86–94, https://doi.org/10.1111/j.1574-6968.2009.01738.x.
[33] C. Wyre, T.W. Overton, J. Ind. Microbiol. Biotechnol. 41 (2014) 1391–1404, https://doi.org/10.1007/s10295-014-1489-1.
[34] P. Dvorak et al., Microb. Cell Fact. 14 (2015) 201, https://doi.org/10.1186/s12934-015-0393-3.
[35] N. Kronqvist et al., Nat. Commun. 8 (2017) 15504, https://doi.org/10.1038/ncomms15504.
[36] A. Abelein et al., Sci. Rep. 10 (1) (2020), https://doi.org/10.1038/s41598-019-57143-x.
[37] M. Sarr et al., FEBS J. 285 (2018) 1873–1885, https://doi.org/10.1111/febs.14451.
[38] E.H. Abdelkader, G. Otting, J. Biotechnol. 325 (2021) 145–151, https://doi.org/10.1016/j.jbiotec.2020.11.005.
[39] G. Chen et al., Nat. Commun. 8 (2017) 2081, https://doi.org/10.1038/s41467-017-02056-4.
[40] J.H. Choi, K.C. Keum, S.Y. Lee, Chem. Eng. Sci. 61 (2006) 876–885, https://doi.org/10.1016/j.ces.2005.03.031.
[41] M. Merlin et al., Biomed. Res. Int. 2014 (2014) 1–14, https://doi.org/10.1155/2014/136419.
[42] J. Kopp et al., Bioeng. Biotechnol. 8 (2020) 1312. https://doi.org/10.3389/fbioe.2020.573607.
[43] G. Greco et al., Molecules 25 (2020) 3248, https://doi.org/10.3390/molecules25143248.
[44] G. Greco et al., Commun. Mater. 2 (2021) 43, https://doi.org/10.1038/s43246-021-00147-w.
[45] F. Müller, S. Zainuddin, T. Scheibel, Molecules 25 (2020) 5540, https://doi.org/10.3390/molecules25235540.
[46] J. Johansson, A. Rising, ACS Nano 15 (2021) 1952–1959, https://doi.org/10.1021/acsnano.0c08933.
[47] C.S. Shin et al., Biotechnol. Prog. 13 (1997) 249–257, https://doi.org/10.1021/bp970018m.
[48] T.W. Kim, B.H. Chung, Y.K. Chang, Biotechnol. Prog. 21 (2005) 524–531, https://doi.org/10.1021/bp049645j.
[49] F. Xu et al., Nanotechnology 25 (2014) 325701, https://doi.org/10.1088/0957-4484/25/32/325701.
[50] Y. Yang et al., Mater. Sci. Eng. C 107 (2020) 110197, https://doi.org/10.1016/j.msec.2019.110197.

Supplementary Information

High-yield production of a super-soluble miniature spidroin for biomimetic high-performance materials

Benjamin Schmuck[a], Gabriele Greco[b,c,] Andreas Barth[d], Nicola M. Pugno[b,e], Jan Johansson[a], and Anna Rising[a,c*]

[a]*Department of Biosciences and Nutrition, Karolinska Institutet, Neo, 141 86 Huddinge, Sweden*

[b]*Laboratory of Bionic, Nano, Meta, Materials & Mechanics, Department of Civil, Environmental and Mechanical Engineering, University of Trento, Via Mesiano, 77, 38123 Trento, Italy*

[c]*Department of Anatomy, Physiology and Biochemistry, Swedish University of Agricultural Sciences, Uppsala, Sweden*

[d]*Department of Biochemistry and Biophysics, Svante Arrhenius väg 16C, Stockholm University, 10691 Stockholm, Sweden*

[e]*School of Engineering and Materials Science, Queen Mary University of London, Mile End Road, London E1 4NS, UK*

*Corresponding author: anna.rising@ki.se

Materials and Methods

Fed-batch cultivation of E. coli. A day culture of BL21 (DE3) transformed with pT7-NT2RepCT (batch 150I, 150I_2, 200I, 250I, 150IL) was grown in LB-medium (50 µg/ml Kanamycin) at 37°C and 160 rpm until the OD_{600} was 5. Then the culture was diluted 100 times into a sterilized Multifors 2 (0.5 l single-walled glass vessel, Infors HT, Basel, Switzerland), or a BioBench Modular (3 l single-walled glass vessel, Solida Biotech, Munich, Germany), filled with 250 ml or 1 l, respectively, of semi-complex medium according to da Silva and coworkers [1]. Da Silva et al. describe the exact composition of the batch medium we have used in all our cultivations in experiment #4. The cultivation medium was prepared by first autoclaving the main components in the reaction vessel, followed by separate addition of sterile stock solutions of filtered glucose (700 g/l) and kanamycin (50 mg/ml), as well as autoclaved antifoam 204 (10%, Sigma Aldrich), trace metal solution (25x), and $MgSO_4$ (245 g/l). The kanamycin concentration was 50 µg/ml in all cultivations, and the initial concentration of antifoam 204 was 0.005%, which was increased when needed. The pH was continuously adjusted to 7, by the addition of either 3M H_3PO_4 or 25 % NH_3. The oxygenation level pO_2 was set to 30%, which was controlled by increasing the stirrer speed (200-1200 rpm) and/or the airflow rate.

After inoculation, the bioreactor cultures were grown at 25°C before the temperature was decreased to 20°C when OD_{600} reached 50 (batch 150I, 150I_2, 200I, 250I). Then, protein expression was induced with IPTG (batch 150I: 150 µM; batch 150I_2: 150 µM; batch 200I: 200 µM; batch 250I: 250 µM). The larger cultivation (batch 150IL) was grown at 29°C until OD_{600} approached 60, then slowly chilled to 20°C, before it was induced with 150 µM IPTG when the OD_{600} was 77.

Exponential feeding with a semi-complex medium (also defined by da Silva and co-workers in experiment #4) containing 40% glycerol (batch 150I) or 70% glycerol (batch 150I_2, 200I, and 250I) was triggered automatically once the initial C-source was depleted, indicated by a sudden increase of pO_2. The feeding rate was adjusted to an exponential feeding profile according to equation (1):[2]

$$F = \frac{1}{S} * \left(\frac{\mu}{Y_{X/S}} + m\right) * X_0 * e^{\mu t} \qquad (1)$$

Where F is the rate of feeding (l h^{-1}), S the concentration of the glycerol in the feed (g l^{-1}), µ the specific growth rate (h^{-1}), $Y_{X/S}$ the biomass yield on the substrate (g g^{-1}), m the specific maintenance coefficient (g g^{-1} h^{-1}), X the biomass concentration (g l^{-1}). The specific growth rate

μ was set to 0.1, m to 0.025 g g^{-1} h^{-1}, and $Y_{X/S}$ was 0.622 g g^{-1}[1]. To minimize the risk for excessive glycerol accumulation because of the longer cultivation time after induction for batch 150I_2, 200I, and 250I, the exponential feed was aborted after 6 h. Instead, the culture was fed with a constant feeding profile. Maximal 125 ml feeding solution was added to cultivations using the Multifors 2 bioreactor.

Batch 150IL, cultivated using the BioBench Modular system, was fed with the same semi-complex medium as batch 150I, but using a linear increase feeding profile from 11 to 30 ml/h for 10h, and then continuing with a constant feed rate until 500 ml were consumed. Feeding was also triggered once the initial C-source was depleted, indicated by a sudden increase of pO_2.

The cultures were harvested 22h (batch 150I & 150 IL) or 36 h (batch 150I_2, 200I, and 250I) post-induction by centrifugation at 4,000 x g, the supernatant was discarded, and 20 ml Buffer T (20 mM Tris-HCl, pH 8) per 10 g wet cell pellet was used for resuspension using gentle agitation at 6°C and 100 rpm. The cell resuspension was stored at -20°C until further processed.

Purification of NT2RepCT. The cell pellet was thawed and diluted with buffer T to approximately 2.5 mg NT2RepCT/ml, before DNAse I (Roche, Basel, Switzerland) was added to a concentration of 10 μg/ml. Then cell lysis was performed with a Cell disruptor (Constant Systems, Daventry, United Kingdom) at 30 kPSi and 4°C. Next, the lysed cells were centrifugated at 25,000 x g for 45 min at 4°C to remove insoluble debris. The cell lysate was filtered through a 0.45 μm Filtropur S (Sarstedt, Nümbrecht, Germany) before loading the sample with an Äkta Explorer liquid chromatographic system (GE Healthcare, Uppsala, Sweden) at 6°C onto Ni-NTA columns, either one Hisprep FF 16/10 20 ml column (5 ml/min) or on four sequentially coupled 5 ml HiTrap Chelating HP columns (3.5 ml/min). After loading ~ 150 ml lysate (around 400 mg protein), the column was washed with 75 ml TB. Subsequently, the column was washed with TB containing 2 mM imidazole (90 ml), and finally, NT2RepCT was eluted with 200 mM imidazole (40 ml).

The automated purification procedure mentioned in the main text was programmed with the Unicorn 5.1 (GE Healthcare) method editor. Up to 2.5 l cell lysate was processed by incrementally loading 250 ml (10 times) onto 2 sequentially coupled 20 ml IMAC (HisPrep FF 16/10) column at 5 ml/min, using the loop function. During each cycle, the column was first washed with 140 ml TB, and subsequently with 160 ml TB containing 2 mM imidazole. Finally,

NT2RepCT was eluted with 80 ml of buffer TB containing 200 mM imidazole. After each round, the column was re-equilibrated with 3 column volumes buffer TB. The entire process was controlled with a script and did therefore not require any hands-on time. Protein eluate from the same batch, but after several rounds of loading and eluting was collected at 4°C and dialyzed overnight against buffer T using a Spectra Por membrane (Spectrum Labs, Rancho Dominguez, USA) with a molecular weight cut-off between 6-8000 kDa. Purified NT2RepCT was saved at -20°C.

SDS-PAGE and protein quantification. To estimate the concentration of the expressed protein in the bioreactor culture (referred to as expression level in the main text), the culture sample was first centrifuged to pellet the cells. The supernatant was removed, and the sample was diluted 40-times in water, unless noted otherwise. The protein contents of the bioreactor samples were analyzed together with already purified NT2RepCT serving as standards with SDS-PAGE using a 4−20% Mini-protean TGX stain-free precast gel (Bio-Rad, Munich, Germany). The standard consisted of a 2-fold dilution series of NT2RepCT from 1.8 mg/ml to 0.225 mg/ml (concentration determined measuring the absorbance at 280nm, see below). With the software Image lab (Bio-Rad, Munich, Germany), the band intensities corresponding to NT2RepCT were integrated, to create a standard curve correlating band intensity to concentration.

The dry cell weight of culture 150IL was determined by adding 1 ml of cell resuspension (in triplicates) to dried and weighed Eppendorf tubes. The cells were pelleted by centrifugation, the supernatant was removed, and the pellet was dried at 65°C for at least 24h, until the weight was stable. GelAnalyzer 19.1[3] was used to estimate the % of NT2RepCT relative to the total protein amount, using the scanned SDS-PAGE gels. Finally, assuming a protein fraction of 55% relative to the total dry cell mass [4] the expression level could be calculated, to confirm the results from the quantification method using NT2RepCT standards.

The purity of the purified NT2RepCT was assessed with SDS-PAGE. The concentration and the total yield (referred to as yield after purification in the main text) was calculated after measuring absorbance at 280 nm in triplicates (using a 10- time dilution), using the protein-specific extinction coefficient of 18,910 M^{-1} cm^{-1}, obtained with the ProParam tool available via the Expasy server [5].

Biomimetic spinning of NT2RepCT. The protein preparation was concentrated to 300 mg/ml with an Amicon Ultra-15 centrifugal filter unit (Merck-Millipore, Darmstadt, Germany)

equipped with an ultracel-10 membrane (10 kDa cutoff) at 4,000 x g and 4°C. Biomimetic spinning of NT2RepCT was done as described earlier by Greco et. al [3], with the exception that the fibers were collected in air on frames attached to a wheel (diameter 11 cm) placed at the end of an 80 cm spinning bath and 80 rpm (46 cm s^{-1}).

Tensile Testing. The mechanical properties of the fibers from batch 150I and 250I were determined with tensile tests exactly as described previously [6]. Values reported in this study represent an average of tensile tests from 20 individual fibers for each sample. Since the humidity affects the mechanical properties of the fibers [7], the fibers were tested at relative humidity lower than 30% and a temperature of 19-21 °C. The average fiber diameter of each fiber subjected to tensile tests was determined by taking three representative images in an optical microscope at 10x magnification. The reported diameter is the average of three fiber width measurements, which was done for each image taken. The fiber cross-sectional area for the derivation of the mechanical properties was calculated assuming a circular cross-section. This leads to an underestimation of the calculated stress of fibers that had non-circular, e.g., a dumbbell-shaped cross-section (Figure S5).

We also performed tensile tests in the same way on the following reference fibers: Kevlar Technora T240_440dtex fibers (Teijin) and Carbon C T24-5.0/270-E100 fibers (SGL). Before tensile testing, the fibers were fixed in a 1x1 cm paper frame window with super glue.

Scanning Electron Microscopy (SEM). For the SEM characterization, we used a field emission FE-SEM (Zeiss – 40 Supra). The metallization was made by using a sputtering machine Quorum 150T and the sputtering mode was Pt/Pd 80:20 for 5 minutes.

Fourier Transform Infrared (FTIR) spectroscopy. FTIR spectra were obtained on fiber bundles with a Vertex 70 equipped with a Platinum-ATR and an MeCdTe-detector (Bruker, Ettlingen, Germany) according to the method described by Greco et. al [6]. For each fiber type, six spectra were recorded. To obtain information on the β-sheet content of the fibers, the spectra were averaged, the baseline was subtracted, and the spectrum was fitted with the Kinetics software by E. Goormaghtigh (Université Libre de Bruxelles, Belgium), as described earlier by Gonska et. al [8]. The average absorbance spectrum and its second derivative of the amide I region (1700−1600 cm^{-1}) were co-fitted, meaning that they were fitted simultaneously in order to get a better defined fit (see **Figure S7D**) [9]. In this fitting procedure, we used a

Savitzky−Golay window of 17, 19, and 21 points, and the weighting factor of the second derivative was 300. The average secondary structure content the standard deviation are reported. The secondary structure content was calculated from the relative band areas of the component bands. At ∼1598 cm^{-1} the component band was assigned to amino acid side chain absorbance. At ∼1696, ∼1637, ∼1625, and at ∼1614 cm^{-1} the component bands were assigned to β- sheets. The component bands at ∼1654 cm^{-1} was assigned to α-helix/random structures and that at ∼1672 cm^{-1} to turns. The component band fitted at ∼1684 cm^{-1} was assigned to β-sheet/turns, and therefore excluded from the calculation of the β-sheet content, due to the ambiguity of the assignment.

Table S1. Summary of the bioreactor cultivation parameters.

Culture	150l	150l_2	200l	250l	150lL
Temperature (BI/AI)[a]	25/20	25/20	25/20	25/20	29/20
Feed	40% Glycerol	70% Glycerol	70% Glycerol	70% Glycerol	40% Glycerol
Feed volume (ml)	125	125	125	125	500
IPTG conc (μM)	150	150	200	250	150
OD_{600} induced	50	51	52	51	77
OD_{600} harvest	156	108	90	142	204
Total induction time (h)	22	36	36	36	21
Culture size at harvest (ml)	352	350	339	343	1600
Wet cell weight (g/l)	214	142	138	201	301[d]
Expression level (g/l)[b]	13.2	12.2	9.4	15.9	20.9[e]
% culture used on IMAC	100%	9%	27%	47%	41%
Purified from IMAC (mg)	3915	248	653	1839	9642
Yield after purification (g/l)[c]	**11.1**	**7.6**	**7.1**	**11.3**	**14.5**
% of max exp. protein	84%	63%	76%	71%	70%

a) Before induction (BI), after induction (AI). b) The expression level of NT2RepCT was estimated with SDS-PAGE using already purified NT2RepCT as the standard. c) Refers to the amount of purified NT2RepCT in gram that was obtained from each liter of culture. The purity of the purified NT2RepCT was assessed with SDS-PAGE (for instance **Figure S5**), and the concentration was determined by measuring the absorbance at 280 nm and using the protein-specific extinction coefficient of 18,910 M^{-1} cm^{-1}. d) Dry cell weight was determined to 80 g/l. e) Considering the dry cell weight, a protein content of 55% compared to the total dry weight, and determining the % of NT2RepCT relative to the total protein content (**Figure S4**), an expression level of 20.8 g/l was calculated.

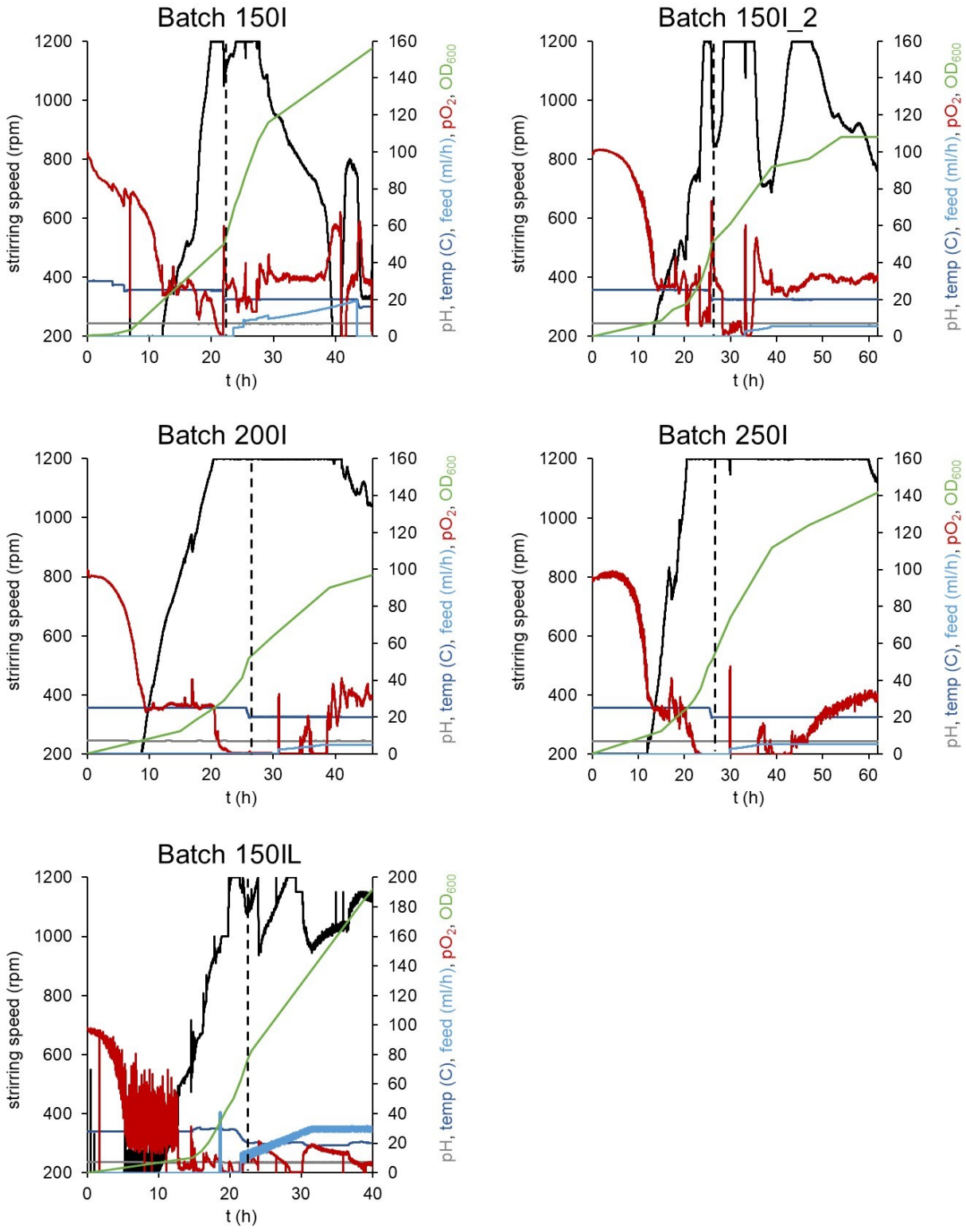

Figure S1. Parameters during a bioreactor cultivation of batch 150I, 150I_2, 200I, 250I, and 150IL. The stirring speed (black), pO_2 (red), pH (grey), temperature (dark blue), feeding rate (light blue), and the optical cell density (green) are shown. The induction point is indicated by a black dashed line.

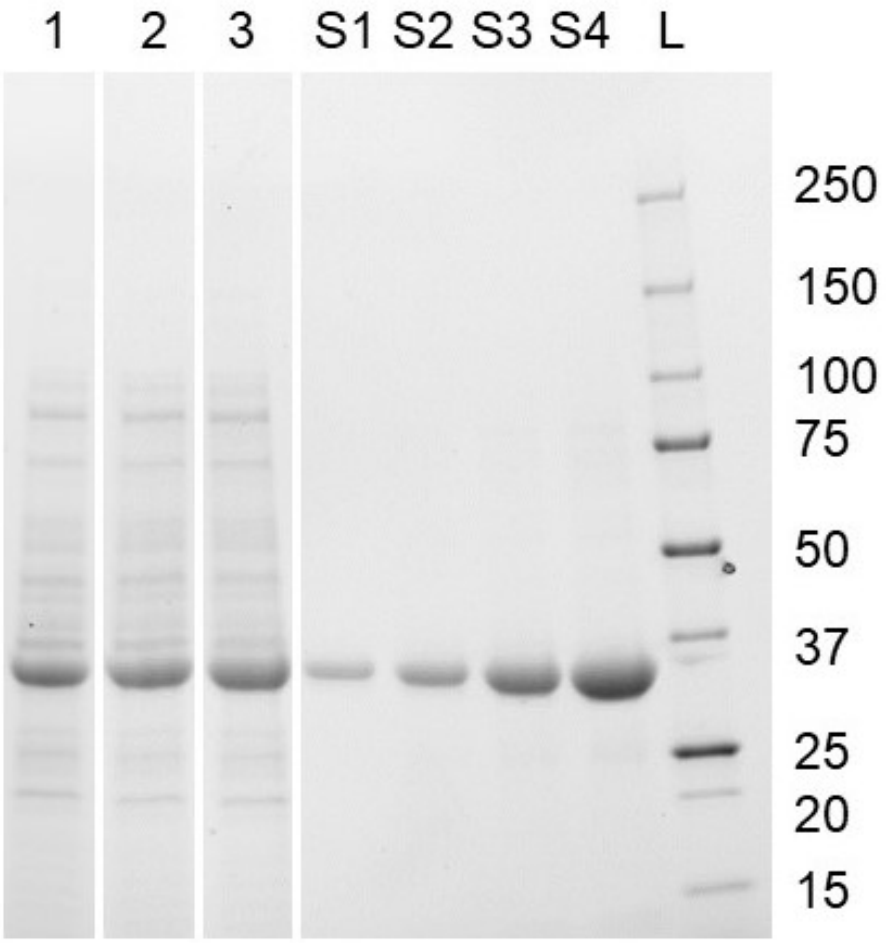

Figure S2. SDS-PAGE of samples from a fed-batch cultivation of *E. coli* BL21 overexpressing NT2RepCT in a bioreactor. The samples (1-3) were obtained 36 h after induction with 150 µM (1), 200 µM (2), or 250 µM (3) IPTG and diluted 20-fold. 225, 450, 900, and 1800 µg/ml of already purified NT2RepCT (S1-S4) was used to estimate the NT2RepCT concentration in sample 1-3, by peak integration of the bands using the software Image Lab (Bio-Rad). (L) Protein size ladder, the molecular masses (kDa) of the bands are indicated to the right.

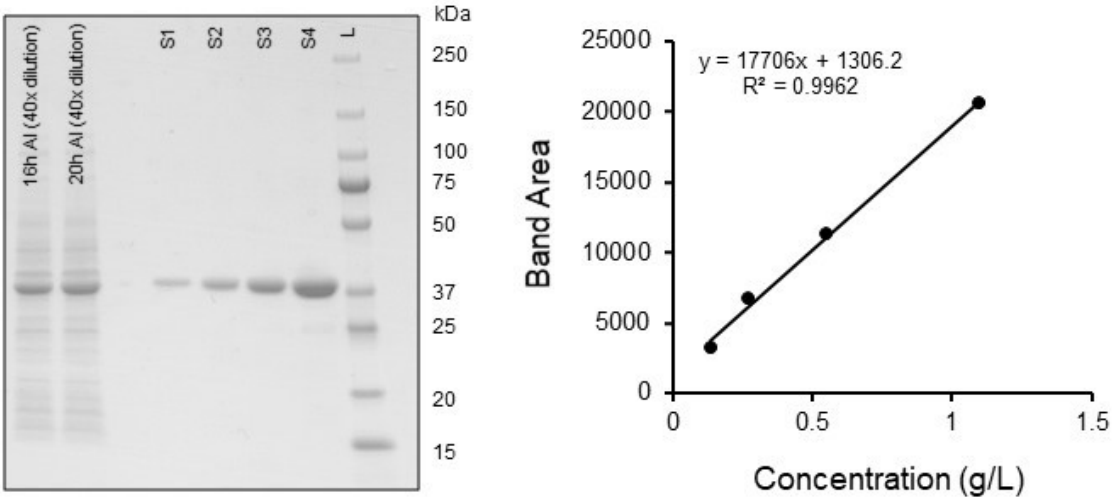

Figure S3. SDS-PAGE of samples from a fed-batch cultivation of *E. coli* BL21 overexpressing NT2RepCT in a 3 l bioreactor (batch 150IL). The samples representing the total cell content were obtained 16h or 20h after induction (AI) and diluted 40-fold. The two-fold dilution series (S1-S4, 137 – 1100 µg/ml) of already purified NT2RepCT was used to estimate the NT2RepCT concentration in the culture samples, by peak integration of the bands using the software Image J. (L) Protein size ladder, the molecular masses (kDa) of the bands are indicated to the right. The linear dependency of band area as a function of the concentration using the standards is shown in the plot on the right-hand side.

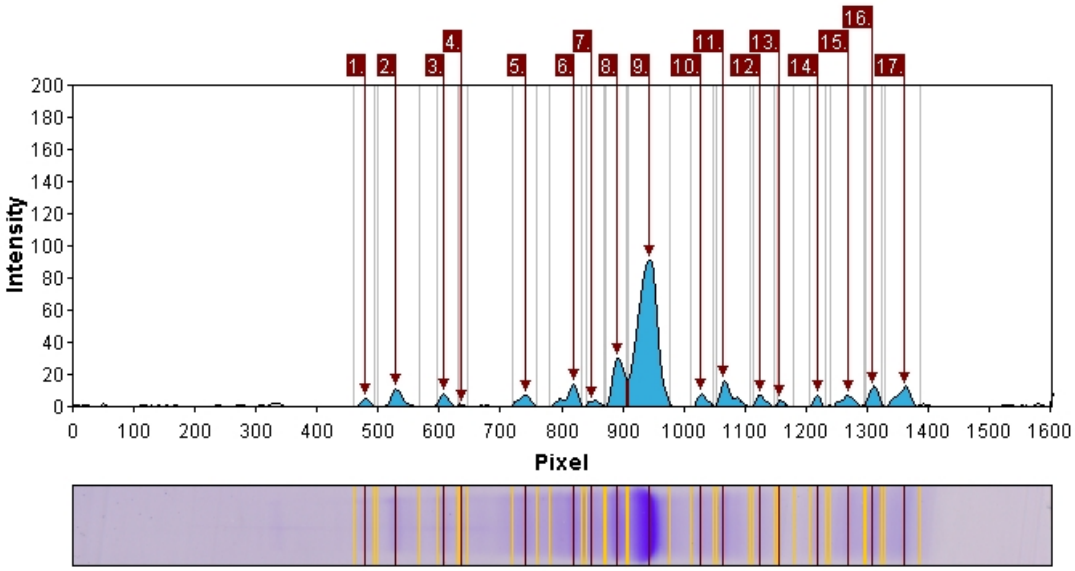

Figure S4. The NT2repCT content in % relative to the total protein content was determined with GelAnalyzer 19.1 [3]**.** Shown here is the lane profile of band 20h AI (40x dilution) from **Figure S3** (batch 150IL). NT2RepCT accounts for 52% of the total protein.

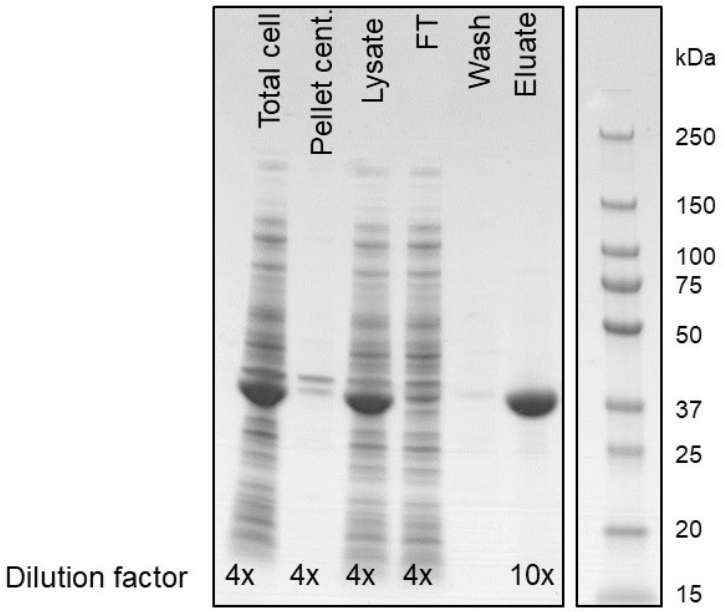

Figure S5. SDS-PAGE of the purification of NT2RepCT (batch 150IL), using the Äkta Explorer liquid chromatographic system, and a Hisprep FF 16/10 (20 ml) column. Total Cell: Cell suspension before cell lysis. Pellet cent.: Insoluble debris after cell lysis and centrifugation. Lysate: Supernatant after centrifugation. FT: Flow through after loading the lysate onto the column. Wash: The column was washed with 2 mM imidazole to remove weakly bound proteins. Eluate: NT2RepCT released from the column after elution with 200 mM imidazole.

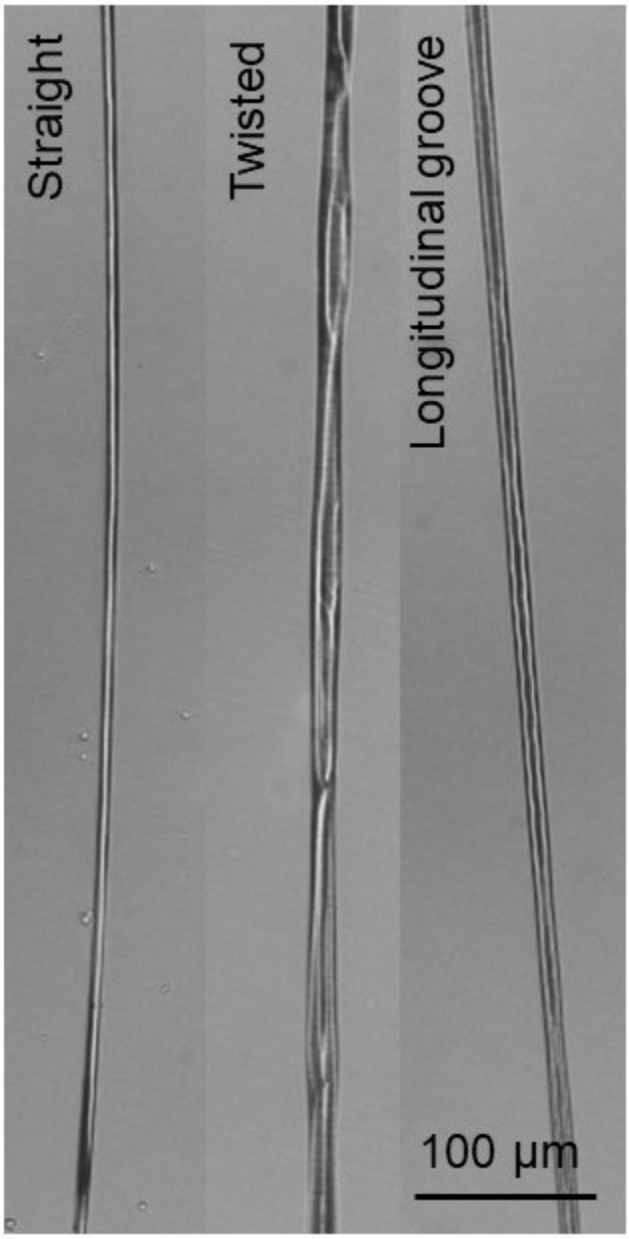

Figure S6. Representative micrographs of fibers spun from NT2RepCT expressed in batch 150I using light microscopy at 10x-fold magnification. Representative images are shown to illustrate the three different morphological types observed. Fibers appeared to be either straight, had a twisted appearance, or exhibited a longitundinal groove. In a sample of 20 randomly selected fibers, about 65% appeared straight, 20% exhibited the longitudinal groove, and 15% had a twisted appearance.

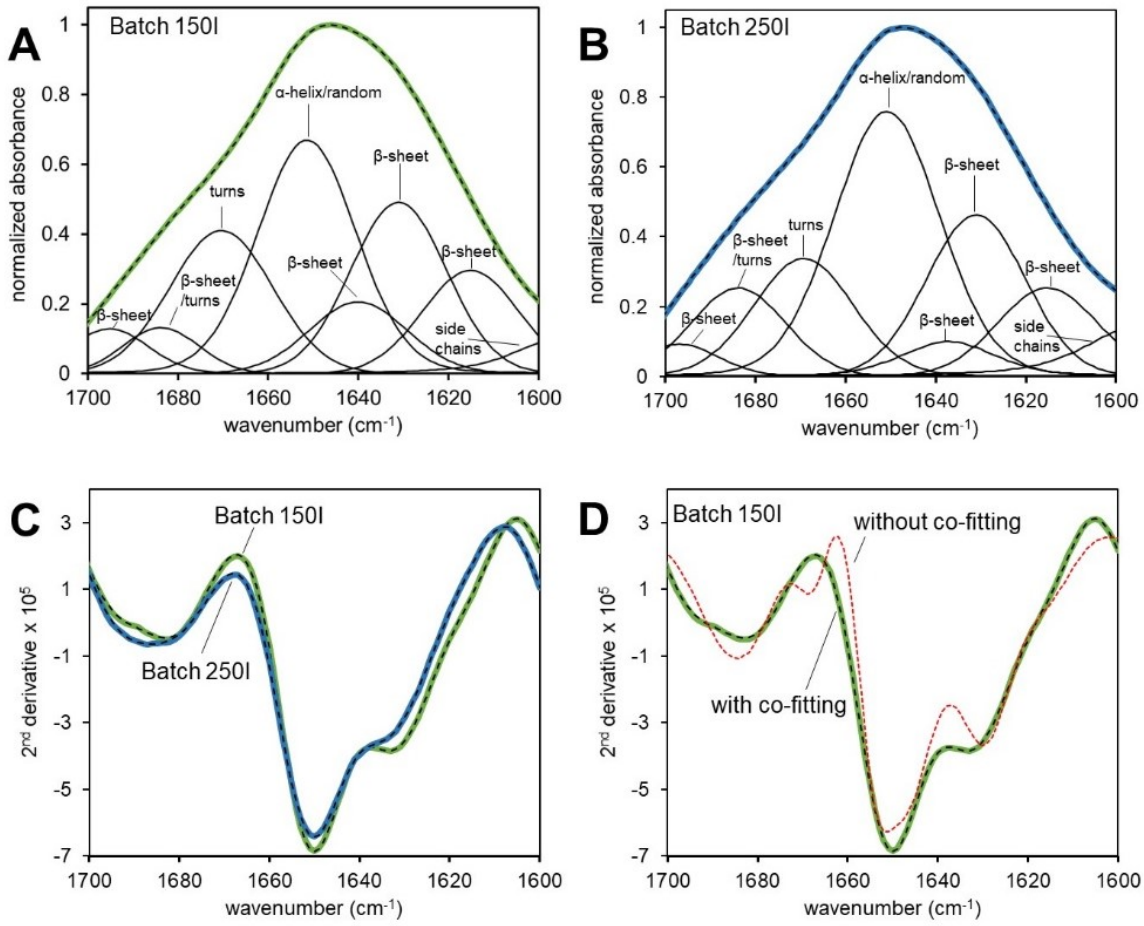

E

secondary structure element	batch 150I	batch 250I
beta-sheet (%)	42.5 ± 2.0	37.9 ± 1.6
alpha-helix/disordered (%)	29.4 ± 2.6	29.2 ± 3.8
turns (%)	15.2 ± 3.4	16.1 ± 2.2

Figure S7. (A) A) Deconvolution of the amide I region of the FTIR spectra of biomimetic silk fibers spun with NT2RepCT purified from batch 150I (green), according to a method that simultaneously fits the absorbance spectrum and its second derivative [9]. This is advantageous because more spectral information is considered to generate the fit, which is therefore better defined [9]. The fit model (black dashed line) consisted of the minimum number of component bands (black lines) that were necessary to describe the second derivative spectra. (B) Same as (A) but showing NT2RepCT fibers from batch 250I (blue) and the corresponding fit (black dashed line). (A & B) The deconvolution and fitting shown here were obtained using a Savitzky−Golay window of 19 points, and the weighting factor of the second derivative was 300. The assignments of the individual component bands are indicated. (C) The second derivatives of the normalized absorbance spectra in the amide I region (green: batch 150I; blue: batch 250I) and the corresponding fits are indicated by black dashed lines. (D) Illustrates the difference between the co-fitting procedure (green line: second derivative of the absorbance spectrum; black dashed line: corresponding fit) and using only the absorbance spectrum for fitting (red dashed line). The experimental second derivative spectrum is clearly better reproduced by co-fitting than by fitting only the absorbance spectrum, which demonstrates that co-fitting better takes into account the available spectral information. (E) The relative secondary structure content of NT2RepCT fibers from batch 150I and 250I.

References

[1] A.J. da Silva, A.C.L. Horta, A.M. Velez, M.R.C. Iemma, C.R. Sargo, R.L.C. Giordano, M.T.M. Novo, R.C. Giordano, T.C. Zangirolami, Springerplus 2 (2013) 1–12.

[2] L. Strandberg, FEMS Microbiol. Rev. 14 (1994) 53–56.

[3] GelAnalyzer 19.1 (www.gelanalyzer.com) by Istvan Lazar Jr., PhD and Istvan Lazar Sr., PhD, CSc

[4] Y.X. Yang, Z.G. Qian, J.J. Zhong, X.X. Xia, Process Biochem. (2016).

[5] E. Gasteiger, C. Hoogland, A. Gattiker, S. Duvaud, M.R. Wilkins, R.D. Appel, A. Bairoch, in: J.M. Walker (Ed.), Proteomics Protoc. Handb., Humana Press, Totowa, NJ, 2005, pp. 571–607.

[6] G. Greco, J. Francis, T. Arndt, B. Schmuck, F.G. Bäcklund, A. Barth, J. Johansson, N.M. Pugno, A. Rising, Molecules 25 (2020) 3248.

[7] G. Greco, T. Arndt, B. Schmuck, J. Francis, F.G. Bäcklund, O. Shilkova, A. Barth, N. Gonska, G. Seisenbaeva, V. Kessler, J. Johansson, N.M. Pugno, A. Rising, Commun. Mater. 2 (2021) 43.

[8] N. Gonska, P.A. López, P. Lozano-Picazo, M. Thorpe, G. V. Guinea, J. Johansson, A. Barth, J. Pérez-Rigueiro, A. Rising, Biomacromolecules 21 (2020) 2116–2124.

[9] M. Baldassarre, C. Li, N. Eremina, E. Goormaghtigh, A. Barth, Molecules 20 (2015) 12599–12622.